Resonance Energy Transfer in Cells: A New Look at Fixation Effect and Receptor Aggregation on Cell Membrane

Max Anikovsky,* Lianne Dale,† Stephen Ferguson,† and Nils Petersen*‡
*Department of Chemistry, University of Alberta, Edmonton, Alberta; †Robarts Research Institute, London, Ontario; and ‡National Institute for Nanotechnology, National Research Council Canada, Edmonton, Alberta, Canada

ABSTRACT Fluorescence resonance energy transfer (FRET) measurements offer a reliable and noninvasive approach to studying protein and lipid colocalization in cells. We have considered systems in which FRET occurs as intramolecular and/or intermolecular process. The proposed dynamic FRET model shows that in the case of intermolecular process the degree of aggregation only slightly affects the energy transfer efficiency. The theory was tested on a set of donor-acceptor pairs in which energy transfer occurs intramolecularly, intermolecularly, or both. The obtained experimental results are in a good agreement with the proposed model. It is well known that the energy transfer efficiency depends both on the distance between the donor and acceptor molecules and the relative orientation of their respective transition dipole moments. This dual dependence often leads to ambiguity. In this article, we show how FRET efficiency can be significantly reduced even in highly coupled system through conformational restrictions in the donor-acceptor pair. Importantly, such restrictions can be imposed on the system by cell fixation, a procedure routinely used when conducting FRET measurements.

INTRODUCTION

While it is generally accepted that proteins interact with each other in functionally important ways (1,2), how and where these interactions take place is not fully understood. Optical and fluorescence microscopy have proved particularly useful in determining the location of protein complexes and the colocalization of different proteins. However, the optical resolution of most microscopes is subject to the diffraction limit at approximately one-half the wavelength of the light source, which is much larger than the nearest-neighbor distances among interacting proteins. Fluorescence resonance energy transfer (FRET) provides information about protein interactions at the molecular scale and it is possible to perform FRET experiments in an image mode to get information about where the molecular interactions occur within the cellular compartments. Thus, FRET has evolved into a powerful tool for probing intermolecular interaction in living cells such as the degree of protein-protein interaction (3,4), protein complex formation (5), and associations of proteins into dimers or aggregates of higher order (6). FRET can also reveal conformational changes within a single molecular entity (7,8).

FRET measurements aiming to reveal the degree of protein-protein interaction in a cell membrane system have been an area of extensive research in the past years. Different theoretical FRET models considering energy transfer efficiencies in clustered and randomly distributed molecules have been developed (9–16). We believe that it is helpful to compare the extent of energy transfer between donors and acceptors attached to different proteins to that measured between donors and acceptors attached to the same proteins. In this article, we develop a model in which comparison of energy transfer measured in three different systems provides an estimate of the extent of protein-protein interaction. The model extracts the degree of protein-protein aggregation from comparison of intramolecular energy transfer efficiency in covalently linked donor-acceptor pair, intermolecular and intramolecular energy transfer efficiency in covalently linked donor-acceptor pairs coupled with a receptor, and intermolecular energy transfer efficiency in nonlinked donor and acceptor individually coupled with a receptor.

The FRET efficiency is a parameter that measures proximity of two fluorescent molecules in a donor-acceptor pair. FRET efficiency values are determined indirectly from intensity measurements. In the case of imaging, the raw data for FRET analysis are a set of (confocal) images of donor and acceptor fluorescence. These images are processed according to defined algorithms that yield the energy transfer efficiency, which in turn is interpreted in terms of the distance between the molecules or their relative orientation. The accuracy of FRET calculations and their interpretation depends on how well the algorithms are built and how well the assumptions hold. Since energy transfer efficiency depends on both the distance between the donor and acceptor and relative orientation of their transitional dipole moments, ambiguity in interpretation is inherent.

One common assumption is that the relative spatial orientation of the donor and acceptor pair is determined by rapid and isotropic reorientation. This fixes the orientation factor, κ to a known value. Clearly, if there are restrictions to the molecular motion, this assumption is invalid. In this article, we show that fixation of cells with paraformaldehyde reduces the energy transfer efficiency even in chemically linked

Submitted October 23, 2007, and accepted for publication March 7, 2008.

Address reprint requests to Nils Petersen, Tel.: 780-641-1610; E-mail: nils.petersen@nrc-cnrc.gc.ca.

Editor: Michael Edidin.

© 2008 by the Biophysical Society
0006-3495/08/08/1349/11 $2.00

doi: 10.1529/biophysj.107.124313

systems of chromophores, presumably because their relative motions become restricted.

In some of the model FRET systems used in the article, the corticotropin releasing factor (CRF) type 1α receptor was fused to donor and acceptor. CRF belongs to subfamily B of G-protein coupled receptors (GPCR), which in turn constitutes a large family of integral membrane protein receptors. Ligand binding to GPCRs initiates an intracellular signal pathway through activation of G-proteins. CRF receptors in particular are believed to play a key role in stress response and in mediating anxiety and depressive disorders (17,18). These receptors remain the main target for many therapeutic drugs, since they play a crucial role in many physiological processes (19). The current belief is that they exist and function as dimeric entities or aggregates (20). As is the case with many other GPCRs, CRF type 1α receptors associate within the membrane (21). Here we determine the extent of self-association using receptors labeled with cyan fluorescence protein (CFP) and yellow fluorescence protein (YFP) as well as receptors labeled with CFP-YFP or YFP-CFP constructs.

MODEL FOR DEPENDENCE OF FRET EFFICIENCY ON DEGREE OF AGGREGATION

The energy transfer efficiency measured in a particular system can given by

$$\Theta_{\mathrm{FRET}} = \frac{I_{\mathrm{donor}} - I_{\mathrm{donor-acceptor}}}{I_{\mathrm{donor}}}, \tag{1}$$

where $I_{\mathrm{donor\text{-}acceptor}}$ and I_{donor} are the relative donor fluorescence intensities in the presence and absence of acceptor, respectively.

Let us assume that the donor and acceptor exist in the form of aggregates of a single kind (dimers ($n = 2$), trimers ($n = 3$), tetramers ($n = 4$), etc.) and the probability of a donor molecule to form an aggregate with an acceptor molecule is the same as for the donor or acceptor to form aggregates with themselves.

Let n be the degree of aggregation and m be the number of acceptor molecules in an aggregate. Hence, (n-m) is the number of donor molecules in an aggregate. In this case, the number of combinations in which the donor and acceptor form an aggregate can be found through the binomial theorem:

$$(pD + (1-p)A)^{\mathrm{n}} = \sum_{\mathrm{m}=0}^{\mathrm{n}} \frac{n!}{(n-m)!m!} p^{\mathrm{n-m}} (1-p)^{\mathrm{m}} D^{\mathrm{n-m}} A^{\mathrm{m}}. \tag{2}$$

Here, p is the probability of getting a donor molecule when randomly choosing from the population. In other words, p is a concentration factor representing donor-acceptor ratio in the system. The values D and A in Eq. 2 are dimensionless symbols representing donor and acceptor molecules, respectively.

To illustrate how Eq. 2 works, let us consider the cases of dimer and trimer formation when the concentrations of donor and acceptor are the same. This would correspond to the value of p equal 0.5.

For dimers, Eq. 2 takes the form

$$(0.5D + 0.5A)^2 = 0.25DD + 2 \times 0.25DA + 0.25AA. \tag{2a}$$

The coefficients found in the right part of Eq. 2a represent the probability of finding a particular molecular combination upon aggregation. Thus, according to Eq. 2a, approximately one-quarter of the dimer population should be formed by donor molecules only (DD combination), another quarter should comprise dimers containing acceptor molecules only (AA combination), and half of the dimers will be formed by donor and acceptor molecules (DA combination). It is crucial to understand that this statistical distribution only works if the probability of forming a dimer is the same between all molecular entities present in the system.

For trimers, Eq. 2 takes the form

$$(0.5D + 0.5A)^3 = 0.125DDD + 3 \times 0.125DDA + 3 \times 0.125DAA + 0.125AAA. \tag{2b}$$

In this case, the probability of finding a trimer formed by three donor molecules (DDD combination) or three acceptor molecules (AAA combination) equals 0.125 while the probability of finding a trimer formed by two donor molecules and one acceptor molecule (DDA combination) or one donor molecule and two acceptor molecules (DAA combination) equals 0.375. Thus, for equal donor and acceptor concentrations, approximately one-eighth of trimer population will be formed by donor molecules only, another one-eighth by acceptor molecules only; three-eighths by two donor molecules and one acceptor molecule; and the rest three-eighths of the population, by one donor molecule and two acceptor molecules.

Consequently, the system will comprise three different ensembles in case of dimerization and four different ensembles in case of trimer formation. These ensembles have different energy transfer efficiencies and the relative amount of each ensemble in the system depends on the donor-acceptor concentration ratio. Thus, these ensembles will contribute differently to the overall FRET efficiency measured in the experiment.

Now let us consider donor fluorescence intensities in different ensembles in the absence and presence of acceptor. Let i_{D} be the donor intensity per donor from an ensemble without energy transfer or quenching. In the presence of energy transfer (ET), the donor intensity will be reduced by a factor of $(1 - \varphi_{\mathrm{ET}}^{\mathrm{D^{n-m}...A^m}})$, where $\varphi_{\mathrm{ET}}^{\mathrm{D^{n-m}...A^m}}$ is the energy transfer efficiency in that particular ensemble which is formed by m acceptor molecules and n-m donor molecules (see Table 1 for details). Summing up the donor fluorescence intensities in the presence and absence of acceptor from Table 1 and substituting them into Eq.1 with appropriate concentration

TABLE 1 Donor intensities in different ensembles in the presence and absence of energy transfer as a function of donor-acceptor concentrations and the degree of aggregation

Aggregation state	Ensemble	FRET efficiency	Combination	Concentration coefficient	Donor intensity	
					In the absence of acceptor	In the presence of acceptor
Dimer	1	0	DD	p^2	$2i_D$	$2i_D$
	2	$\varphi_{ET}^{D^1\ldots A^1}$	DA	$p(1-p)$	i_D	$i_D(1-\varphi_{ET}^{D^1\ldots A^1})$
	2	$\varphi_{ET}^{D^1\ldots A^1}$	AD	$p(1-p)$	i_D	$i_D(1-\varphi_{ET}^{D^1\ldots A^1})$
	3	0	AA	$(1-p)^2$	0	0
Trimer	1	0	DDD	p^3	$3i_D$	$3i_D$
	2	$\varphi_{ET}^{D^2\ldots A^1}$	DDA	$p^2(1-p)$	$2i_D$	$2i_D(1-\varphi_{ET}^{D^2\ldots A^1})$
	2	$\varphi_{ET}^{D^2\ldots A^1}$	DAD	$p^2(1-p)$	$2i_D$	$2i_D(1-\varphi_{ET}^{D^2\ldots A^1})$
	2	$\varphi_{ET}^{D^2\ldots A^1}$	ADD	$p^2(1-p)$	$2i_D$	$2i_D(1-\varphi_{ET}^{D^2\ldots A^1})$
	3	$\varphi_{ET}^{D^1\ldots A^2}$	AAD	$p(1-p)^2$	i_D	$i_D(1-\varphi_{ET}^{D^1\ldots A^2})$
	3	$\varphi_{ET}^{D^1\ldots A^2}$	ADA	$p(1-p)^2$	i_D	$i_D(1-\varphi_{ET}^{D^1\ldots A^2})$
	3	$\varphi_{ET}^{D^1\ldots A^2}$	DAA	$p(1-p)^2$	i_D	$i_D(1-\varphi_{ET}^{D^1\ldots A^2})$
	4	0	AAA	$(1-p)^3$	0	0

coefficients (Table 1), the overall FRET efficiency can be calculated for the systems of aggregates of different order. In particular, in the case of dimer formation,

$$\Theta_{FRET} = (1-p)\varphi_{ET}^{D^1\ldots A^1},$$

where $\varphi_{ET}^{D^1\ldots A^1}$ is FRET efficiency in the dimer formed by one donor and one acceptor molecule.

In the case of trimer formation,

$$\Theta_{FRET} = 2p(1-p)\varphi_{ET}^{D^2\ldots A^1} + (1-p)^2\varphi_{ET}^{D^1\ldots A^2},$$

where $\varphi_{ET}^{D^2\ldots A^1}$ and $\varphi_{ET}^{D^1\ldots A^2}$ are FRET efficiencies in trimers formed by two donor—one acceptor molecules and one donor—two acceptor molecules, respectively.

The same logic can be extended to aggregates of higher orders and a general formula can be generated as

$$\Theta_{FRET} = \sum_{m=1}^{n-1} B_{m+1}\frac{(n-m)p^{(n-m)}(1-p)^m}{np}\varphi_{ET}^{D^{n-m}\ldots A^m}, \quad (3)$$

where Θ_{FRET} energy transfer efficiency measured in the system comprised by the aggregates of a single kind which are formed by different number of donor and acceptor molecules, B_{m+1} is the binomial coefficients (in case of dimer $B_1 = 1$, $B_2 = 2$, $B_3 = 1$), n is the degree of aggregation, m is the number of acceptor molecules in an ensemble, and $\varphi_{ET}^{D^{n-m}\ldots A^m}$ is the energy transfer efficiency of an ensemble.

Thus, Eq. 3 defines the overall FRET efficiency measured in the system through energy transfer efficiencies of ensembles that constitute the system.

Resonance energy transfer is a competitive process leading to deactivation of the donor excited state. We now consider systems in which energy transfer occurs intramolecularly, intermolecularly, or when both intra- and intermolecular processes are present.

For the system in which the donor and acceptor are parts of one molecular entity (Fig. 1 *A*), the energy transfer efficiency can be expressed as

$$\varphi_{ET}^{D-A} = \frac{k_{intra}^{D-A}c_{intra}^{A}}{k_\Sigma + k_{intra}^{D-A}c_{intra}^{A}}. \quad (4)$$

Here, φ_{ET}^{D-A} is the energy transfer efficiency in the system where the donor and acceptor are covalently linked together. I.e., FRET occurs intramolecularly, $k_{intra}^{D-A}$is the rate constant of intramolecular energy transfer, k_Σ is the sum of rate constants of all the processes that compete with energy transfer (such as internal conversion, intersystem crossing, radiative decay), and c_{intra}^{A} is the effective concentration of the acceptor molecules that participate in the intramolecular energy transfer.

In the system where both intramolecular and intermolecular energy transfer are possible (see Fig. 1 *B* for the case when dimers are formed), the energy transfer efficiency is given by

$$\varphi_{ET}^{(D-A)_n} = \frac{k_{intra}^{D-A}c_{intra}^{A} + k_{inter}^{D\ldots A}c_{inter}^{A}}{k_\Sigma + k_{intra}^{D-A}c_{intra}^{A} + k_{inter}^{D\ldots A}c_{inter}^{A}}, \quad (5)$$

where c_{inter}^{A} is the effective concentration of the acceptor molecules that participate in the intermolecular energy transfer and $k_{inter}^{D\ldots A}$ is the rate constant of intermolecular energy transfer.

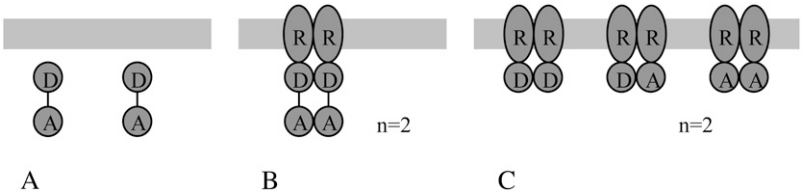

FIGURE 1 Schematic representation of the systems in which intermolecular (*A*), both inter- and intramolecular (*B*), and intermolecular-only (*C*) energy transfers occur.

Finally, we are going to consider the system that consists of several ensembles with different energy transfer efficiencies and in which only intermolecular energy transfer is possible. The case when the system comprises dimers is considered in Fig. 1 *C*.

The energy transfer efficiency for each of the ensembles is given by

$$\varphi_{ET}^{D^{n-m}\ldots A^m} = \frac{k_{inter}^{D\ldots A}(c_{inter}^{A})_m}{k_\Sigma + k_{inter}^{D\ldots A}(c_{inter}^{A})_m}, \quad (6)$$

where $(c_{inter}^{A})_m$ is the effective acceptor concentration in an ensemble containing m acceptor molecules and $k_{inter}^{D\ldots A}$ is the rate constant of intermolecular energy transfer in the nonlinked system assumed to be the same as in Eq. 5.

One may note that c_{inter}^{A}, and $(c_{inter}^{A})_m$ are interrelated with c_{intra}^{A}. Indeed, if one donor molecule is covalently linked with one acceptor molecule and such FRET system is capable of forming an aggregate in which intermolecular energy transfer becomes possible along with intramolecular process, then the effective concentrations can be expressed as

$$c_{inter}^{A} = (n-1) \times c_{intra}^{A}, \quad (7)$$

where n is a degree of aggregation (Fig. 1 *B*).

In the case of dimer, three different ensembles are present in the system. However, the energy transfer only occurs in ensemble 2, which is formed by one donor molecule and one acceptor molecule (Fig. 1 *C* and Table 1). For this ensemble, the effective acceptor concentration $(c_{inter}^{A})_1$ is the same as the effective acceptor concentration in the case of intramolecular energy transfer c_{intra}^{A} since, in both cases, each donor molecule can transfer energy to one acceptor molecule.

In the case of trimer, there are four different ensembles in the system (Table 1) and only ensembles 2 and 3 contribute to the energy transfer process.

In ensemble 2, two donor molecules are associated with one acceptor molecule, i.e., the effective acceptor concentration is the same as in the case of intramolecular energy transfer $(c_{inter}^{A})_1 = c_{intra}^{A}$. In ensemble 3, one donor molecule is associated with two acceptor molecules and the effective acceptor concentration $(c_{inter}^{A})_2$ is twice as high as the effective acceptor concentration in the case of intramolecular energy transfer c_{intra}^{A}, i.e., $(c_{inter}^{A})_2 = 2 \times c_{intra}^{A}$.

Thus, the effective concentration of acceptor in an ensemble containing m acceptor molecules can be expressed as

$$(c_{inter}^{A})_m = m \times c_{intra}^{A}. \quad (8)$$

Solving Eqs. 4–8, one can find the expected energy transfer efficiency for different ensembles in different states of aggregations.

For the only ensemble that contributes to the energy transfer process in case of dimerization, the energy transfer efficiency is given by

$$\varphi_{ET}^{D^1\ldots A^1} = \frac{\varphi_{ET}^{(D-A)_2} - \varphi_{ET}^{D-A}}{(1-\varphi_{ET}^{(D-A)_2})(1-\varphi_{ET}^{D-A}) + (\varphi_{ET}^{(D-A)_2} - \varphi_{ET}^{D-A})}.$$

For ensemble 2 (DDA combination), in the case of trimer formation, the energy transfer efficiency is given by

$$\varphi_{ET}^{D^2\ldots A^1} = \frac{\varphi_{ET}^{(D-A)_3} - \varphi_{ET}^{D-A}}{2(1-\varphi_{ET}^{(D-A)_3})(1-\varphi_{ET}^{D-A}) + (\varphi_{ET}^{(D-A)_3} - \varphi_{ET}^{D-A})}.$$

For ensemble 3 (DAA combination), in the case of trimer formation, the energy transfer efficiency is given by

$$\varphi_{ET}^{D^1\ldots A^2} = 2\frac{\varphi_{ET}^{(D-A)_3} - \varphi_{ET}^{D-A}}{2(1-\varphi_{ET}^{(D-A)_3})(1-\varphi_{ET}^{D-A}) + 2(\varphi_{ET}^{(D-A)_3} - \varphi_{ET}^{D-A})}.$$

The same logic can be extended to ensembles formed by aggregates of higher orders and a general formula for the energy transfer efficiency expected from each ensemble can be derived

$$\varphi_{ET}^{D^{n-m}\ldots A^m} = \sum_{m=1}^{n-1} \frac{m \times (\varphi_{ET}^{(D-A)_n} - \varphi_{ET}^{D-A})}{(n-1)(1-\varphi_{ET}^{(D-A)_n})(1-\varphi_{ET}^{D-A}) + m \times (\varphi_{ET}^{(D-A)_n} - \varphi_{ET}^{D-A})}. \quad (9)$$

Substituting Eq. 9 into Eq. 3, we obtain the expression for the energy transfer efficiency expected to be measured in the experiment in the system where FRET occurs intermolecularly:

$$\Theta_{FRET} = \sum_{m=1}^{n-1} B_{m+1} \frac{(n-m)p^{(n-m)}(1-p)^m}{np} \frac{m \times (\varphi_{ET}^{(D-A)_n} - \varphi_{ET}^{D-A})}{(n-1)(1-\varphi_{ET}^{(D-A)_n})(1-\varphi_{ET}^{D-A}) + m \times (\varphi_{ET}^{(D-A)_n} - \varphi_{ET}^{D-A})}. \quad (10)$$

Equation 10 shows that the efficiency of intermolecular energy transfer is a function of degree of aggregation, relative concentration of donor and acceptor, and energy transfer efficiencies in donor-acceptor pairs where FRET occurs both intra- and intermolecularly ($\varphi_{ET}^{(D-A)_n}$) and intramolecularly only

(φ_{ET}^{D-A}). We used Eq. 10 to generate FRET efficiency curves for different values of $\varphi_{ET}^{(D-A)_n}$ and φ_{ET}^{D-A}. The results are presented in Fig. 2. Interestingly, intermolecular energy transfer shows very slight dependence on the degree of aggregation in the entire range of aggregation numbers when $\varphi_{ET}^{(D-A)_n}$ and φ_{ET}^{D-A} are comparable in values. When $\varphi_{ET}^{(D-A)_n}$ is significantly higher than φ_{ET}^{D-A}, intermolecular FRET increases noticeably only in the range of low aggregation numbers ($n = 2$–4).

To test the theory we conducted FRET measurements in three different systems. The first system comprised a covalently linked donor-acceptor pair (CFP-YFP) (Fig. 1 *A*). We demonstrate here that, in this system, energy transfer occurs intramolecularly only. The second system comprised the same covalently linked donor-acceptor pair (CFP-YFP) fused with a cell membrane receptor (CRF type 1α receptor). Receptor aggregation on cell surface may open an additional intermolecular energy transfer channel. In this case, donor can transfer its energy not only to the acceptor it is linked to but also to the acceptor that belongs to a different molecular entity (Fig. 1 *B*). Finally, FRET was measured in the system where only intermolecular energy transfer is possible. In this system, CRF receptor was covalently linked to either donor or acceptor and FRET was measured between donor and acceptor brought together by the receptor aggregation, as illustrated in Fig. 1 *C*.

MATERIALS AND METHODS

Materials

Human embryonic kidney (HEK) 293 cells were obtained from the American Type Culture Collection (ATCC, Manassas, VA). Tissue culture reagents and Lipofectamine 2000 were purchased from Invitrogen/Molecular Probes (Burlington, ON, Canada). Extinction coefficient 26,000 M^{-1} cm^{-1}, fluorescence quantum yield 0.4 (ECFP-N1) and extinction coefficient 36,500 M^{-1} cm^{-1}, fluorescence quantum yield 0.63 (EYFP-N1) were used as energy transfer donor and acceptor, respectively (BDBiosciences/Clontech, Palo Alto, CA).

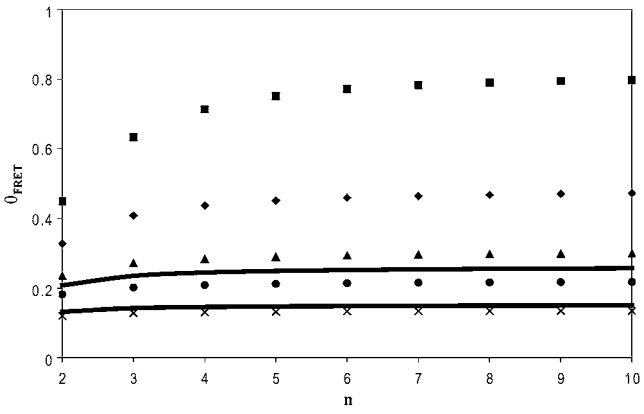

FIGURE 2 Dependence of intermolecular FRET efficiency on degree of aggregation. The curves were generated using Eq. 10 for equal concentrations of donor and acceptor and different values of $\varphi_{ET}^{(D-A)_n}$ and φ_{ET}^{D-A}: $\varphi_{ET}^{(D-A)_n} = 0.9$, $\varphi_{ET}^{D-A} = 0.1$ (*squares*); $\varphi_{ET}^{(D-A)_n} = 0.7$, $\varphi_{ET}^{D-A} = 0.3$ (*diamonds*); $\varphi_{ET}^{(D-A)_n} = 0.5$, $\varphi_{ET}^{D-A} = 0.1$ (*triangles*); $\varphi_{ET}^{(D-A)_n} = 0.5$, $\varphi_{ET}^{D-A} = 0.3$ (*circles*); and $\varphi_{ET}^{(D-A)_n} = 0.3$, $\varphi_{ET}^{D-A} = 0.1$ (*crosses*). The solid curves were calculated using $\varphi_{ET}^{(D-A)_n}$ and φ_{ET}^{D-A} values from the experimental FRET data in Table 3 for the SE method. The upper curve corresponds to the CFP-YFP coupled and uncoupled systems ($\varphi_{ET}^{(D-A)_n} = 0.6$, $\varphi_{ET}^{D-A} = 0.44$); the bottom curve corresponds to the YFP-CFP coupled and uncoupled systems ($\varphi_{ET}^{(D-A)_n} = 0.46$, $\varphi_{ET}^{D-A} = 0.33$).

Plasmid constructs

Cyan fluorescence protein (CFP)-yellow fluorescence protein (YFP) and YFP-CFP fusions were generated by inserting CFP or YFP without a stop codon into a frame with the existing YFP or CFP found in the pEYFP-N1 (pECFP-N1) vectors (BDBiosciences/Clontech) at the *Bam*HI and *Eco*RI sites. PCR was used to remove the stop codon from CFP or YFP and introduce *Bam*HI and *Eco*RI sites at the appropriate places to ensure that the CFP or YFP without the stop codon was inserted in the correct reading frame. Analogously, CRF1α-CFP-YFP fusion was generated by inserting CFP into existing CRF1α-YFP vector (22) at *Bam*HI and *Eco*RI sites. To engineer CRF1α-YFP-CFP, PCR was used to remove the stop codon from YFP with pEYFP-N1 used as a template and introduce *Eco*RI and *Bam*HI sites first. Then, CRF1α was subcloned from CRF1α-YFP in pECFP-N1 to create CRF1α-CFP. Finally, the PCR product was subcloned in frame into CRF1α-CFP to create CRF1α-YFP-CFP fusion protein. The constructs were verified by restriction analysis.

Cell culture, transfection, and fixation

HEK293 cells were cultured in Eagle's minimal essential medium containing fetal bovine serum (10% v/v) as well as penicillin/streptomycin. For confocal imaging, cells were split into 35-mm glass-bottom dishes and proliferated until they reached 90% confluency. Transfection was conducted using Lipofectamine 2000 according to the manufacturer's instructions. To fix the transfected cells they were incubated for 20 min at room temperature in 3.7% paraformaldehyde diluted in 1× PBS.

Confocal microscopy

Confocal imaging was performed on a Leica TSC SP2 (Leica Microsystems, Richmond Hill, ON, Canada) laser-scanning confocal microscope using 63× oil immersion objective. Transfected HEK293 cells were maintained in 1× PBS at 37°C on a heated stage. Argon laser lines of 458 nm and 514 nm were used as excitation sources for CFP and YFP, respectively. Emission was detected in the following spectral windows: 465–485 nm (CFP) and 550–570 nm (YFP).

FRET measurements

There are two common steady-state experimental approaches to measuring FRET in cells: acceptor (photo)bleaching (AB); and sensitized (acceptor) emission (SE). Both techniques are based on the fact that FRET causes the fluorescence intensity of the donor to decrease and the fluorescence intensity of the acceptor to increase due to the transfer of energy from the donor to the acceptor. The AB method measures the amount of donor emission decrease while the SE method measures the growth of acceptor emission. Both assume that other experimental parameters, such as donor and acceptor fluorescence quantum yields and spectral detection efficiencies, are known.

We employed both the AB and SE methods to obtain FRET data. All our FRET experiments were performed on the Leica TSC SP2 confocal microscope and the algorithms for conducting the experiments were developed with the system capabilities in mind. The Leica TSC SP2 combines confocal microscopy imaging with spectrophotometric detection that enables fluorescence detection in the regions where there is no contamination from crosstalk (or its contribution to the signal in question is negligible (23)). In all the

experiments, CFP and YFP were used as the donor and acceptor of energy, respectively.

AB approach

In the AB method, the donor fluorescence intensity is measured first in the presence of the acceptor and then in its absence after the acceptor has been photobleached from the system by repeated laser irradiation. The FRET efficiency (Θ_{FRET}) is then calculated according to Eq. 1.

The detection range for the donor emission was chosen to be 465–485 nm (Channel D). The acceptor fluorescence in this region is null, which makes us conclude that all the changes in the emission intensities detected at these wavelengths are due to changes in the donor fluorescence caused by FRET and it is valid to calculate FRET efficiency by substituting the directly measured values in Eq. 1. Since the donor emission extends very far into longer wavelength regions and overlaps with the acceptor emission spectrum at almost all wavelengths, it is impossible to pick up a detection region where the acceptor emission would be clear from the donor bleedthrough signal and at the same time significantly higher than a noise level. The spectral window 550–570 nm (Channel A) chosen to monitor the amount of the acceptor bleached is a good compromise between the detection efficiency and the amount of the donor fluorescence contaminating the signal. The experiments were terminated when no further changes in the acceptor intensities were observed. When acquiring the donor images, the excitation laser power and detector sensitivity were optimized to obtain an image of high quality and at the same time to minimize bleaching of the donor. The donor intensities were measured by selecting region of interest within the collected image before and after bleaching. FRET efficiency was calculated using Eq. 1 and the final value was the average from 20 different images.

One of the advantages of the AB approach is that it offers quantitative FRET measurements without the need to introduce parameters that correct for microscope properties. On the other hand, the AB technique relies on the photobleaching being complete and it does not take into account the fact that photochemical reactions initiated by repeated laser irradiation may, in principle, produce highly reactive species that will cause the destruction of donor molecules. Thus, the AB approach can lead to an underestimate of the FRET efficiency.

SE approach

The SE method relies on measuring an increase in the acceptor fluorescence when the donor is introduced into the system. For the CFP-YFP donor-acceptor pair, the acceptor emission is always contaminated by the donor fluorescence and, therefore, it is technically more challenging to conduct SE measurements. The experiment requires determination of a number of control parameters that account for the amount of fluorescence detected in the acceptor channel due to emission of the donor, as well as the amount of fluorescence detected in the acceptor channel due to direct excitation of the acceptor with the donor excitation wavelength. Different approaches have been developed to obtain all of the necessary values (24–26). In all of them, single and double-labeled specimens are required and a linear dependence of fluorescence intensities between single- and double-labeled samples is assumed. These approaches are only valid for particular levels of sensitivity (27), so caution is required when adopting these methods.

The SE method allows for eliminating all the hardware limitations that one could potentially face in AB. The amount of FRET in an acceptor signal contaminated with cross-talk can be assessed based on the assumption that fluorescence intensities in single- and double-labeled specimens are linearly related.

The SE approach for our FRET experiments was specifically developed with the Leica hardware capabilities in mind. In general, the total intensity in the acceptor detection channel is a sum of three contributions: intrinsic acceptor fluorescence due to direct excitation; donor bleedthrough into the acceptor channel; and the FRET signal, if present. The first two signals can be neglected only if the acceptor is not excited by the donor excitation wavelength and the emission spectrum of the donor does not extend into the acceptor detection channel or the donor fluorescence quantum yield is negligible. Under our experimental conditions, that is not the case, and the overall intensity I_A measured in channel A is

$$I_A = I^{458}_{a(d+a)A} + I^{458}_{d(d+a)A} + I_{FRET\,A}, \tag{11}$$

where $I^{458}_{a(d+a)A}$ is the acceptor fluorescence intensity in channel A due to direct excitation with the donor wavelength in the sample where both the donor and acceptor are present, $I^{458}_{d(d+a)A}$ is donor bleedthrough signal into channel A in the sample where both the donor and acceptor are present (i.e., the intensity in the acceptor channel arising from donor emission), and $I_{FRET\,A}$ is the FRET signal in channel A, the desired quantity. In all cases, the superscript indicates the excitation wavelength (see Table 2 for a guide to the symbols and their meaning).

In our SE experiments, the amount of the donor bleedthrough into channel A ($I^{458}_{d(d+a)A}$) was evaluated by means of a correction curve (Fig. 3) that was generated using a sample labeled with the donor only. The fluorescence donor intensities in Channel D ($I^{458}_{d(d\,only)D}$) and Channel A ($I^{458}_{d(d+a)A}$) were measured at different laser power and in samples with different concentrations of the donor. The obtained values were plotted and linear dependence over a wide range of concentrations and laser powers was observed (Fig. 3), i.e., $I^{458}_{d(d\,only)A} = k\,I^{458}_{d(d\,only)D}$. When the acceptor is present in the system as well, the fluorescence in channel D is not compromised by its emission. Therefore, the amount of the donor bleedthrough into channel A ($I^{458}_{d(d+a)A}$) can be determined by measuring the fluorescence intensity in channel D ($I^{458}_{d(d+a)D}$) and using this value on the correction curve. One major advantage of using the correction curve is that fluorophore concentration and laser power are eliminated as parameters from determining the amount of donor bleedthrough into the acceptor channel.

Each set of FRET measurements consisted of two steps and was carried out with constant laser intensities and the same PMT detector was used in both channels. Correction for PMT spectral sensitivity was made using the spectral sensitivity chart provided by the detector manufacturer. The experiments and calculations were conducted according to the following algorithm:

Step 1. The fluorescence intensities from the sample labeled with both the donor and acceptor and excited at the donor wavelength (458 nm) were measured in Channel D and Channel A. The intensity in channel A represents the total intensity in Eq. 11. The intensity in Channel D was used to determine the amount of the donor bleedthrough into Channel A with the correction curve shown in Fig. 3. Since the dependence is linear and passes through the origin, the bleedthrough signal was estimated using the slope k,

TABLE 2 Symbols representing fluorescence intensities used in the calculations of FRET efficiencies by SE method

		Channel D 465–485 nm		Channel A 550–570 nm		
	System	Donor intensity	FRET signal	Donor intensity	Acceptor intensity	FRET signal
Donor excitation	Donor only	$I^{458}_{d(d\,only)D}$		$I^{458}_{d(d\,only)A}$		
	Acceptor only				$I^{458}_{a(a\,only)A}$	
	Donor + acceptor		$I_{FRET\,D}$	$I^{458}_{d(d+a)A}$	$I^{458}_{a(d+a)A}$	$I_{FRET\,A}$
Acceptor excitation	Acceptor only				$I^{514}_{a(a\,only)A}$	
	Donor + acceptor				$I^{514}_{a(d+a)A}$	

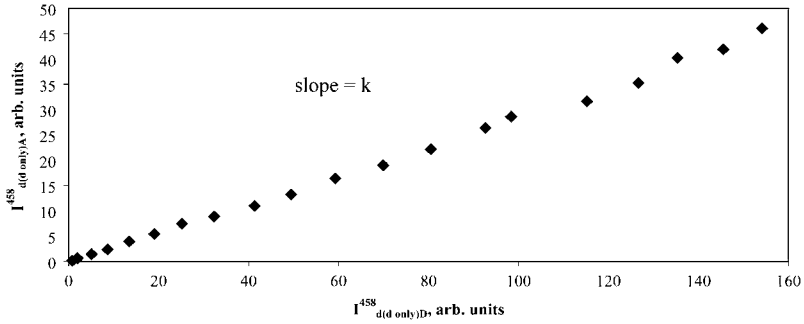

FIGURE 3 Correction curve used to evaluate the amount of donor bleedthrough into the acceptor channel.

$$I^{458}_{d(d+a)A} = k\, I^{458}_{d(d+a)D}, \tag{12}$$

where $I^{458}_{d(d+a)A}$ is the donor bleedthrough into the acceptor channel when both the donor and acceptor are present in the system, and $I^{458}_{d(d+a)D}$ is the donor intensity measured in Channel D from the same sample.

Step 2. To calculate the amount of intrinsic acceptor fluorescence in Channel A due to direct excitation with the donor wavelength, the sample from Step 1 was excited with the acceptor excitation wavelength (514 nm) and the fluorescence of intensity $I^{514}_{a(d+a)A}$ was measured in Channel A. Since the donor is not excited at this wavelength, all the emission detected is due to the acceptor fluorescence from direct excitation. The amount of the acceptor emission in Channel A from excitation with the 514 nm laser line should be proportional to the amount of the acceptor emission in the same channel from excitation with the 458 nm laser line. Thus, the amount of intrinsic acceptor fluorescence in channel A due to direct excitation with the donor wavelength in the sample, where both the donor and acceptor are present can be determined as

$$I^{458}_{a(d+a)A} = \frac{I^{458}_{a(a\,only)A}}{I^{514}_{a(a\,only)A}} I^{514}_{a(d+a)A}. \tag{13}$$

After inserting Eqs. 12 and 13 into Eq. 11, the intensity of FRET signal in channel A is given by

$$I_{FRET\,A} = I_A - k\, I^{458}_{d(d\,only)D} - \frac{I^{458}_{a(a\,only)A}}{I^{514}_{a(a\,only)A}} I^{514}_{a(d+a)A}. \tag{14}$$

The intensity of FRET signal in channel D was determined according to

$$I_{FRET\,D} = I_{FRET\,A} \frac{\varphi_D}{\varphi_A} \frac{\omega_A}{\omega_D}, \tag{15}$$

where φ_D and φ_A are fluorescence quantum yields of the donor and acceptor, and ω_D and ω_A are average spectral sensitivities of the detector in channels D and A, respectively.

Finally, the FRET efficiency was calculated according to

$$\Theta_{FRET} = \frac{I_{FRET\,D}}{I^{458}_{d(d+a)D} + I_{FRET\,D}}, \tag{16}$$

where $I^{458}_{d(d+a)D}$ is the fluorescence intensity measured in Channel D after excitation of a double-labeled sample with the donor excitation wavelength and averaged from 20 different measurements.

RESULTS AND DISCUSSION

After cells were transfected with plasmid DNA and sufficient level of protein expression was reached, a series of confocal images was collected to be then processed according to the two FRET algorithms. In case of the AB approach, an increase in the donor fluorescence intensity was directly observed (Fig. 4, *A* and *C*) after the acceptor was bleached out of the system by continuous irradiation (Fig. 4, *B* and *D*) and the FRET efficiency was calculated using Eq. 1. For SE method, the intensity of FRET signal was obtained from Eq. 15 and the efficiency was calculated using Eq. 16. FRET results for the different systems tested are summarized in Table 3. The error bars were calculated as standard errors of the mean with 95% confidence interval. The sample size for both SE and AB techniques was 20. To check whether the average FRET efficiencies obtained by SE and AB are statistically different, we applied *t*-score analysis to the experimental distributions of measured FRET efficiencies. The calculated *t*-values were compared to the reference values in a standard table of significance with the α-level set at 0.05. The analysis showed that, in most cases, the null hypothesis that the two distributions do not differ from each other cannot be rejected suggesting that the difference between the FRET results obtained by AB and SE methods is statistically insignificant. This supports the equivalence of the two techniques. The only exception was found in the case when the linked donor and acceptor were fused with the receptor. The fact that the values of FRET efficiencies measured by AB and SE methods are different in this case must be a result of some systematic effect(s) that occur(s) in the course of conducting measurements. In this context, one of the observations worth pointing out is that FRET efficiencies obtained by AB method are consistently lower compared to SE method. It seems reasonable to suggest that, in the case of AB, a systematic effect may arise due to the destructive nature of the method itself. Indeed, bleaching of the acceptor out of the system most probably occurs through the generation of reactive oxygen species that, in turn, may result in partial decomposition of the donor. In this case, FRET values appear to be lower compared to the actual ones. We believe that this deviation is more pronounced when the linked CFP and YFP are fused with the receptor because, in this case, in addition to donor molecules which are covalently linked to the acceptor, extra donor molecules belonging to different molecular entities get brought into close proximity of the acceptor molecules. This increases the probability of the donor to be destroyed. As a result, the FRET values determined by the two methods are statistically different in this case.

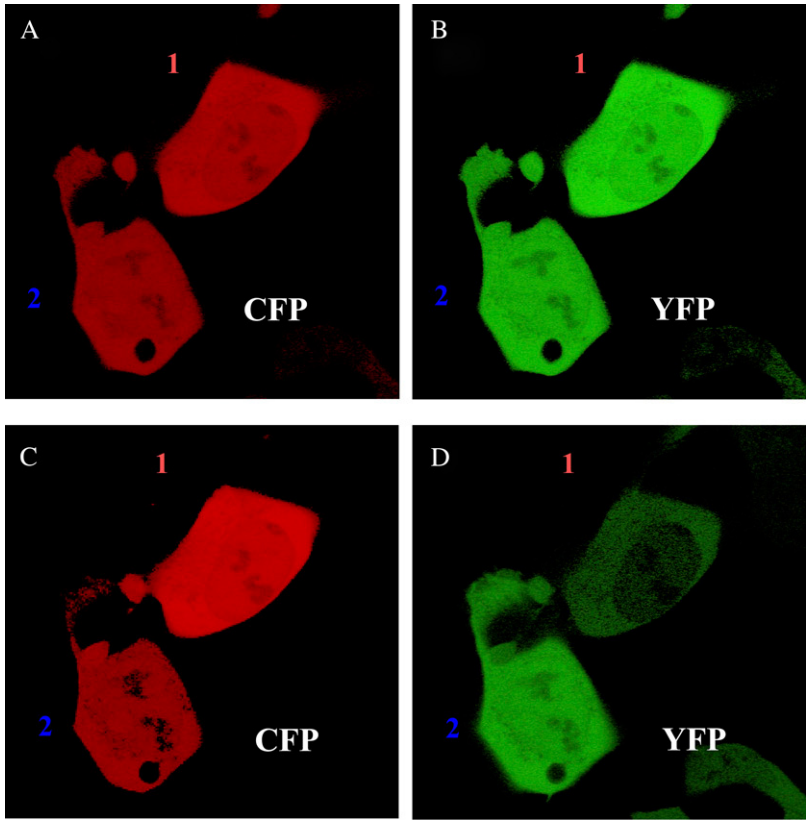

FIGURE 4 HEK 293 cells transfected with CFP-YFP fusion protein. Panels *A* and *C* represent CFP channel before and after bleaching; panels *B* and *D* represent YFP channel before and after bleaching. The acceptor was bleached out of cell 1, and cell 2 was used as a control.

Linked CFP and YFP show intramolecular energy transfer sensitive to fixation

In the cells transfected with nonfused CFP and YPF, no energy transfer was detected. In the absence of acceptor, the donor excited-state lifetime is on the order of several nanoseconds (28). To observe energy transfer in this system, the effective acceptor concentration should be very high. This can be achieved if the donor and acceptor form aggregates or their overall concentration is such that the probability of finding an acceptor molecule in close proximity to a donor molecule during its excited-state lifetime is high enough to make the energy transfer process efficient. Since the FRET level was nil in the system, neither of the above conditions was fulfilled making us suggest that CFP and YFP are mainly present in the cytoplasm in the monomeric form. Though GFP dimerization at high concentrations was previously reported (29) and one could expect similar behavior in CFP and YFP since they are structurally similar to their precursor, we believe that CFP and YFP concentrations in the transfected cells were not high enough to facilitate the process of spontaneous dimer formation.

TABLE 3 FRET efficiencies (%) in live and fixed cells determined by acceptor photobleaching (AB) and sensitized emission (SE) techniques

		Alone		CRF-coupled	
		Live	Fixed	Live	Fixed
CFP + YFP	AB	0	0	14 ± 1	12 ± 1
	SE	0	0	10 ± 1	7 ± 1
CFP-YFP	AB	40 ± 2	13 ± 1	46 ± 2	20 ± 1
	SE	44 ± 2	19 ± 2	60 ± 2	35 ± 2
YFP-CFP	AB	32 ± 1	12 ± 1	36 ± 1	17 ± 1
	SE	33 ± 1	16 ± 1	46 ± 2	23 ± 1

In live cells, the energy transfer efficiency had significant values in the systems where the donor was covalently linked to the acceptor. For CFP-YFP and YFP-CFP fusion proteins it was determined to be ~40 and 30%, respectively (Table 3). Since no oligomerization of CFP and YFP were established in nonfused proteins, FRET detected in the fused systems must be completely due to energy transfer from the donor to acceptor within one molecular entity, i.e., intramolecular energy transfer. It is worth noting that the efficiency of the transfer is sensitive to the order in which the donor and acceptor were introduced into the DNA vector used for cell transfection. In the CFP-YFP FRET pair, the efficiency is higher than in the YFP-CFP fusion. Despite the fact that in both vectors the length of the amino-acid link is the same, the average distance between the fluorophores and/or their relative orientation must be different to give a rise to different energy transfer efficiencies.

We then used the same donor-acceptor ensembles for FRET measurements in the cells fixed with paraformalde-

hyde. A dramatic decrease in the energy transfer efficiencies was found for all fused donor-acceptor pairs (Table 3). When energy transfer occurs by the dipole-dipole interaction mechanism, the rate constant of the process depends on the donor excited-state lifetime in the absence of the acceptor (τ_d), the distance between the donor and acceptor (R), and the Förster radius (R_0), a parameter that defines the distance between the donor and acceptor at which the probability of the energy transfer is half and equals the probability that the donor excited state decays through alternative energy degradation channels (30), i.e.,

$$k_{ET} = \frac{1}{\tau_d}\left(\frac{R_0}{R}\right)^6. \quad (17)$$

The value of the Förster radius depends on many parameters and can be calculated from

$$R_0^6 = \frac{9000(\ln 10)\kappa^2\Phi_D^0}{128\pi^5 N_A n^4}\int_0^\infty I_D(\lambda)\epsilon_A(\lambda)\lambda^4 d\lambda. \quad (18)$$

Here Φ is the fluorescence quantum yield of the donor in the absence of the acceptor, n is the refractive index of the medium (1.4 for aqueous solutions), $\varepsilon_A(\lambda)$ is the molar absorption coefficient of the acceptor, and $I_D(\lambda)$ is the fluorescence intensity of the donor.

According to Eqs. 17 and 18 several factors can be held accountable for less efficient energy transfer. The integral in Eq. 18 denotes a degree of spectral overlap between the donor emission spectrum and acceptor absorption spectrum. In our experiments, no spectral changes in the fluorophores upon fixation were detected, which makes us conclude that the value of the integral was not altered. It is unlikely that the donor fluorescence quantum yield decreases, since no changes in average fluorescence intensity in cells were found. Thus, the observed decrease of FRET efficiency should be either due to an increased distance between the donor and acceptor (parameter R in Eq. 17) or reduced values of the orientation factor (parameter κ^2 in Eq. 18). By definition, κ^2 depends on the average relative orientation of the emission transition moment of the donor and the absorption transition moment of the acceptor during the lifetime of the excited state of the donor, so

$$\kappa^2 = \langle(\cos\theta_{DA} - 3\cos\theta_D\cos\theta_A)^2\rangle, \quad (19)$$

where θ_{DA} is the angle between the donor and acceptor transition moments ($\overline{\mu}_D$ and $\overline{\mu}_A$), and θ_D and θ_A are the angles between these transition moments and the line connecting the centers of the chromophores (Fig. 5). Since the donor and acceptor are covalently linked, it is unlikely that fixation leads to a significantly increased distance between the donor and acceptor. On the other hand, immobilization of the fluorophores by the fixation procedure per se may anchor them in positions that disfavor intramolecular energy transfer. As a result, reduced values of κ^2 lead to less efficient energy transfer.

To our knowledge, this is the first observation of cell fixation affecting the energy transfer process directly. Interestingly, cooling the cells to 4°C does not decrease the energy transfer efficiency so it appears that chemical fixation is required.

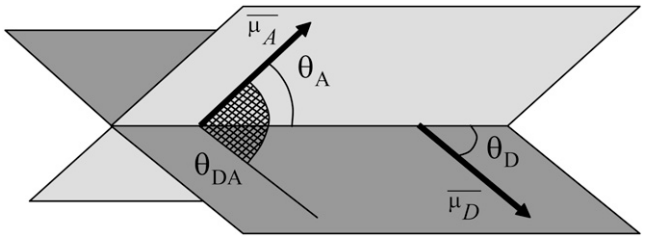

FIGURE 5 Dark-shaded and light-shaded planes represent the planes where transitional dipole moments of the donor and acceptor are located. The values θ_{DA}, θ_D, and θ_A are polar angles used to define relative orientation of the donor and acceptor and calculate the orientation factor κ.

Coupled systems show both intra- and intermolecular energy transfer

In the set of constructs where the CRF receptor was added to the fused CFP-YFP/YFP-CFP proteins (coupled systems), the efficiency of energy transfer was higher compared to the corresponding systems where the donor and acceptor were fused and transfected into the cells without the receptor attached (Table 3). We attribute this increase in the overall FRET efficiency for the CRF-coupled systems to intermolecular energy transfer because of aggregation. An extra energy transfer channel that does not exist in the absence of the receptor is created as a result of interaction of the receptors in the cell membrane. If CRF forms dimers or aggregates of higher order, then such oligomerization will bring donors and acceptors belonging to different molecular entities closer together and that, in turn, will make it possible for the energy transfer to occur intermolecularly as well as intramolecularly. Cotransfection of CRF-CFP and CRF-YFP leads to modest levels of energy transfer. This is consistent with intermolecular ET only.

Intermolecular energy transfer efficiency depends only slightly on the degree of aggregation

Assuming that intramolecular and intermolecular energy transfer are independent processes with rate constants unaffected by each other, they should be treated as competitive paths of energy dissipation in the systems where both are present. Taking into account that the quantum yield of a process depends on its own rate constant and the rate constants of all the competitive processes, we developed a model that considers FRET systems in which the energy transfer occurs intramolecularly, intermolecularly, or both and predicts the amount of intermolecular energy transfer as a function of the degree of aggregation (Eq. 10).

Let us now consider FRET efficiencies obtained experimentally for the systems where the donor and acceptor are linked (intramolecular energy transfer) and the systems where the linked donor and acceptor are coupled with the receptor (intra- and intermolecular energy transfer). For CFP-YFP and YFP-CFP fusion proteins, the energy transfer efficiencies obtained by SE method are 0.44 and 0.33, respectively. For the same fusion proteins coupled with CRF receptor, the energy transfer efficiencies increase up to 0.6 and 0.46. Using these values of FRET efficiencies in Eq. 10 and assuming that the donor and acceptor concentrations are the same, the expected values of intermolecular energy transfer efficiency as a function of the degree of aggregation can be obtained (Fig. 2, *solid curves*). Fig. 2 compares these curves with curves corresponding to several pairs of values of intramolecular energy transfer efficiencies and intra- plus intermolecular energy transfer efficiencies as indicated in the figure caption. As one can see from the figure, the dependence of the energy transfer efficiency on the degree of aggregation is insignificant for our experimental data. If the receptors form dimers, it is estimated to be between 0.13 and 0.2. When the aggregation state changes from a dimer to trimer, the FRET efficiency is expected to be increased on average by $<3\%$ of the dimer value. Further increase in the aggregation number affects the overall efficiency even less and, eventually, FRET levels off, reaching a plateau value.

In the cells cotransfected with CRF-CFP and CRF-YFP vectors, only intermolecular energy transfer is expected to be observed. In this case, ET occurs between the donor and acceptor belonging to two different molecular entities brought together by the receptor aggregation. The measured FRET efficiency in this system determined by SE method was found to be ~ 0.1. This value is slightly lower than the FRET value expected from the system formed by dimers (Fig. 2). It seems fair to suggest that the CRF receptor may not be present in the membrane purely in the dimeric form but rather coexist with monomers in equilibrium. Since the values of FRET efficiency do not show significant dependence on the aggregation state of the receptor (Fig. 2), the aggregates of higher order may potentially be present in the system as well.

Intermolecular energy transfer is not affected by fixation

In the system where the energy transfer occurs only via intermolecular pathway, FRET efficiency shows very slight (if not complete) independence on whether it is measured in live or fixed cells. As one can see from Table 3, in the cells cotransfected with CRF-CFP and CRF-YFP vectors, the energy transfer efficiency values are very close in both live and fixed systems. As mentioned above, fixation has a dramatic effect on the energy transfer efficiency in the linked donor-acceptor pairs. In these systems, a significant decrease in the FRET signal upon fixation is most probably caused by locking the fluorophores in geometrical conformations unfavorable for energy transfer to occur. In live cells, dynamics provides extra degrees of freedom for the linked donor-acceptor pairs, resulting in temporally averaged isotropic distribution of orientations. In the case of the intermolecular energy transfer, a temporally averaged isotropic distribution of orientations caused by dynamics in live cells has the same overall average effect on the energy transfer efficiency as a spatially averaged isotropic distribution of orientations formed upon fixation. This, in turn, suggests that CRF aggregates allow significant flexibility in the orientations (dynamically and spatially) of the fluorophores, and consequently, energy transfer measurements can be reliably done on either live or fixed cells.

In summary, FRET experiments were conducted in the systems where intramolecular and/or intermolecular energy transfer is possible. In all the systems studied, intramolecular component of the energy transfer significantly depends on whether the experiment is conducted in live or fixed cells. This experimentally observed phenomenon can be explained in terms of unfavorable relative geometrical conformation imposed on the donor-acceptor pair by the fixation procedure. Intermolecular component of the energy transfer shows no dependence on fixation.

A new dynamic model considering intra- and/or intermolecular FRET suggests that the energy transfer efficiency only slightly depends on the degree of receptor aggregation.

The work was supported by the Canadian Institute for Photonics Innovation and the Natural Sciences and Engineering Research Council of Canada.

REFERENCES

1. Kretsinger, R. H. 2005. Proteins and the flow of information in cellular function. *In* Molecular Imaging FRET Microscopy and Spectroscopy. A. Periasamy and R. N. Day, editors. Oxford University Press, New York.
2. Giot, L., J. S. Bader, C. Brouwer, A. Chaudhuri, B. Kuang, Y. Li, Y. L. Hao, C. E. Ooi, B. Godwin, E. Vitols, G. Vijayadamodar, P. Pochart, H. Machineni, M. Welsh, Y. Kong, B. Zerhusen, R. Malcolm, Z. Varrone, A. Collis, M. Minto, S. Burgess, L. McDaniel, E. Stimpson, F. Spriggs, J. Williams, K. Neurath, N. Ioime, M. Agee, E. Voss, K. Furtak, R. Renzulli, N. Aanensen, S. Carrolla, E. Bickelhaupt, Y. Lazovatsky, A. DaSilva, J. Zhong, C. A. Stanyon, R. L. Finley, Jr., K. P. White, M. Braverman, T. Jarvie, S. Gold, M. Leach, J. Knight, R. A. Shimkets, M. P. McKenna, J. Chant, and J. M. Rothberg. 2003. A protein interaction map of *Drosophila melanogaster*. *Science*. 302: 1727–1736.
3. Wang, C., W. Bian, C. Xia, T. Zhang, F. Guillemot, and N. Jing. 2006. Visualization of bHLH transcription factor interactions in living mammalian cell nuclei and developing chicken neural tube by FRET. *Cell Res.* 16:585–598.
4. Hebert, T. E., C. Gales, and R. V. Rebois. 2006. Detecting and imaging protein-protein interactions during G protein-mediated signal transduction in vivo and in situ by using fluorescence-based techniques. *Cell Biochem. Biophys.* 45:85–109.
5. Kim, K., D. D. Dimitrova, K. M. Carta, A. Saxena, M. Daras, and J. A. Borowiec. 2005. Novel checkpoint response to genotoxic stress mediated by nucleolin-replication protein A complex formation. *Mol. Cell. Biol.* 25:2463–2474.
6. Storez, H., M. G. H. Scott, H. Issafras, A. Burtey, A. Benmerah, O. Muntaner, T. Piolot, M. Tramier, M. Coppey-Moisan, M. Bouvier,

C. Labbe-Jullie, and S. Marullo. 2005. Homo- and hetero-oligomerization of β-arrestins in living cells. *J. Biol. Chem.* 280:40210–40215.

7. Nakanishi, J., T. Takarada, S. Yunoki, Y. Kikuchi, and M. Maeda. 2006. FRET-based monitoring of conformational change of the β2 adrenergic receptor in living cells. *Biochem. Biophys. Res. Commun.* 343:1191–1196.
8. Mani, R. S., E. V. Usova, C. E. Cass, and S. Eriksson. 2006. Fluorescence energy transfer studies of human deoxycytidine kinase: role of cysteine 185 in the conformational changes that occur upon substrate binding. *Biochemistry.* 45:3534–3541.
9. Shaklai, N., J. Yguerabide, and H. M. Ranney. 1977. Interaction of hemoglobin with red blood cell membranes as shown by a fluorescent chromophore. *Biochemistry.* 16:5585–5592.
10. Fung, B. K., and L. Stryer. 1978. Surface density determination in membranes by fluorescence energy transfer. *Biochemistry.* 17:5241–5248.
11. Wolber, P. K., and B. S. Hudson. 1979. An analytic solution to the Förster energy transfer problem in two dimensions. *Biophys. J.* 28:197–210.
12. Dewey, T. G., and G. G. Hammes. 1980. Calculation of fluorescence resonance energy transfer on surfaces. *Biophys. J.* 32:1023–1035.
13. Yguerabide, J. 1994. Theory for establishing proximity relations in biological membranes by excitation energy transfer measurements. *Biophys. J.* 66:683–693.
14. Veatch, W., and L. Stryer. 1977. The dimeric nature of the gramicidin A transmembrane channel: conductance and fluorescence energy transfer studies of hybrid channels. *J. Mol. Biol.* 113:89–102.
15. Adair, B. D., and D. M. Engelman. 1994. Glycophorin A helical transmembrane domains dimerize in phospholipid bilayers: a resonance energy transfer study. *Biochemistry.* 33:5539–5544.
16. Kenworthy, A. K., and M. Edidin. 1998. Distribution of a glycosylphosphatidylinositol-anchored protein at the apical surface of MDCK cells examined at a resolution of <100 Å using imaging fluorescence resonance energy transfer. *J. Cell Biol.* 142:69–84.
17. Smagin, G. N., and A. J. Dunn. 2000. The role of CRF receptor subtypes in stress-induced behavioral responses. *Eur. J. Pharmacol.* 405:199–206.
18. Merali, Z., L. Du, P. Hrdina, M. Palkovits, G. Faludi, M. O. Poulter, and H. Anisman. 2004. Dysregulation in the suicide brain: mRNA expression of corticotropin-releasing hormone receptors and $GABA_A$ receptor subunits in frontal cortical brain region. *J. Neurosci.* 24:1478–1485.
19. Pierce, K. L., R. T. Premont, and R. J. Lefkowitz. 2002. Seven-transmembrane receptors. *Nat. Rev. Mol. Cell Biol.* 3:639–650.
20. Milligan, G., D. Ramsay, G. Pascal, and J. J. Carrillo. 2003. GPCR dimerization. *Life Sci.* 74:181–188.
21. Kraetke, O., B. Wiesner, J. Eichhorst, J. Furkert, M. Bienert, and M. Beyermann. 2005. Dimerization of corticotropin-releasing factor receptor type 1 is not coupled to ligand binding. *J. Recept. Signal Transd.* 25:251–276.
22. Holmes, K. D., A. V. Babwah, L. B. Dale, M. O. Poulter, and S. S. G. Ferguson. 2006. Differential regulation of corticotropin releasing factor 1α receptor endocytosis and trafficking by β-arrestins and Rab GTPases. *J. Neurochem.* 96:934–949.
23. Calloway, C. B. 2000. A confocal microscope with spectrophotometric detection. *Confocal Microsc.* 4:4–14.
24. Gordon, G. W., G. Berry, X. H. Liang, B. Levine, and B. Herman. 1998. Quantitative fluorescence resonance energy transfer measurements using fluorescence microscopy. *Biophys. J.* 74:2702–2713.
25. Xia, Z., and Y. Liu. 2001. Reliable and global measurement of fluorescence resonance energy transfer using fluorescence microscopes. *Biophys. J.* 81:2395–2402.
26. Chamberlain, C., V. S. Kraynov, and K. M. Hahn. 2000. Imaging spatiotemporal dynamics of Rac activation in vivo with FLAIR. *Methods Enzymol.* 325:389–400.
27. Chen, Y., M. Elangovan, and A. Periasamy. 2005. FRET data analysis: the algorithm. *In* Molecular Imaging FRET Microscopy and Spectroscopy. A. Periasamy and R. N. Day, editors. Oxford University Press, Oxford, UK.
28. Rizzo, M., G. Springer, B. Granada, and D. Piston. 2004. An improved cyan fluorescent protein variant useful for FRET. *Nat. Biotechnol.* 22:445–449.
29. Tsien, R. Y. 1998. The green fluorescent protein. *Annu. Rev. Biochem.* 67:509–544.
30. Forster, Th. Intermolecular energy migration and fluorescence. *Ann. Phys.* 6:55–75.